Published by IOP Publishing for Sissa Medialab

Received: *May 31, 2017*
Accepted: *July 17, 2017*
Published: *August 3, 2017*

International Conference on Instrumentation for Colliding Beam Physics
Budker Institute of Nuclear Physics, Novosibirsk, Russia
27 February – 3 March 2017

2017 JINST 12 C08007

Laser backscattering for beam energy calibration in collider experiments

M.N. Achasov and N.Yu. Muchnoi[1]

[a] *Budker Institute of Nuclear Physics,*
Lavrentieva 11, Novosibirsk, Russian Federation
[b] *Novosibirsk State University,*
Pirogova 2, Novosibirsk, Russian Federation

E-mail: N.Yu.Muchnoi@inp.nsk.su

Abstract: Laser backscattering was implemented as a tool for accurate beam energy measurement at three of the five existing electron-positron colliders. The present report summarizes the experience obtained during these experiments.

Keywords: Gamma detectors (scintillators, CZT, HPG, HgI etc); Instrumentation for particle accelerators and storage rings - high energy (linear accelerators, synchrotrons)

[1] Corresponding author.

© 2017 IOP Publishing Ltd and Sissa Medialab
https://doi.org/10.1088/1748-0221/12/08/C08007

Contents

2017 JINST 12 C08007

1 Introduction

Backscattering of laser radiation on relativistic electrons is clearly associated with the Compton effect, the fundamental process of quantum electrodynamics with accurately established features. With proper selection of a laser source average wavelength of its highly monochromatic radiation may be considered as the constant, known with absolute accuracy at the few ppm level or even better. Hence, the energy spectrum of backscattered photons becomes dependent solely on the electron Lorentz factor $\gamma = E/m$, allowing its accurate determination. Apparently, the first conscious application of this approach was elegantly realised at the Taiwan Light Source [1], where the mean electron beam energy was measured with accuracy of 0.13%. The scattering of CO_2 laser radiation with $\lambda = 10.6\,\mu$m head on the 1.3 GeV electron beam produces narrowly directed backscattered photons with energies up to ~ 3 MeV. At these energies a coaxial HPGe[1] detector has still sufficient total absorption efficiency of few % and excellent energy resolution ($\sim 0.05\%$), which is less or comparable with the energy dispersion of the electrons in the beam. Another essential component of the success is the accurate calibration of the detector energy scale by nuclear radioactive γ-sources. Taken together these conditions impose restrictions on the energies of backscattered photons, which should not exceed 10 MeV or so. Practically it means that with a CO_2 laser radiation the maximum measurable electron energy is limited from above at the level of about 2 GeV. Possible way to overcome this limit within the same approach could be the use of far infrared lasers [2]. Even with this important constraint, application of the method on the other installations did not have long to wait due to its relative simplicity and rather high accuracy. At BESSY-I, II storage rings the precisions of 100 ppm and 30 ppm were achieved [3, 4] for the beam energy measurements at 800 and 1700 MeV, respectively. A substantial increase in measurement accuracy was obtained by more thorough analysis of the energy spectrum of backscattered photons. Due to the large number of existing synchrotron radiation facilities, the application of the approach became widespread, see e.g. [5–7].

[1] High Purity Germanium.

No doubt that beam energy measurement is an attractive opportunity for the experiments with colliding beams. Good knowledge of the c. m. s. energy in lepton colliders had always been a tremendous advantage for precise measurements of particle masses and energy dependencies of cross sections. By now, the application of the laser backscattering for the beam energy determination has been implemented at three colliders: VEPP-4M [8], BEPC-II [9] and VEPP-2000 [10].

At the VEPP-4M collider the beam energy measurement system [11] was commissioned in 2005 on the basis of the ROKK-1M facility [12]. The goal of the system was the continuous monitoring of the beam energy in the long lasting experiment on the τ-lepton mass determination [13]. Since the VEPP-4M collider has a single vacuum chamber for both electrons and positrons, only the energy of electrons was measured. From a methodological point of view, a unique feature of the experiments on the VEPP-4M collider is that there are two completely independent approaches for precise beam energy determination. Application of the resonance depolarization technique [14] had become a routine procedure during the experiments with the KEDR detector [15]. A lot of cross checks were made [16] in order to establish precise energy scale in the energy range of c-τ physics.

In 2010 the first experiment was held with the new beam energy determination system on the BEPC-II collider. This system is more complex, cause it was designed for alternating separate measurements of the beams energies in the electron and positron rings [17–19]. The HPGe detector is installed in the north interaction point of the collider, and the laser beam could be delivered for interaction with either electrons or positrons. Since the laser backscattering is the only method for absolute beam energy calibration at BEPC-II, the necessary cross checks are possible due to precise measurements of J/ψ and $\psi(2S)$ mesons masses [20]. At the BEPC-II collider yet another measurement of the τ-lepton mass was performed in 2011 [21].

The last (in chronological order) beam energy calibration system was commissioned in 2012 at the VEPP-2000 collider [22]. The circumference of this machine is rather small (24.4 m), so it was impossible to find a straight part of the beam orbit for the laser-electron interaction. Therefore quite unusual scheme was realised when the scattering of laser radiation occurs inside the bending magnet. Due to this reason we have observed rather unexpected shape of the energy spectrum of backscattered photons. The explanation however was found soon after the first measurements [23]. It was revealed that such a scheme allows to measure not only the average beam energy and energy spread, but the bending field strength directly in the interaction area.

Detailed descriptions of the systems listed above and examples of their application in physical experiments may be found in the references [11, 17, 19, 23]. In this report we describe the common features of these installations, focusing on the details of the data acquisition and analysis.

2 Absolute measurement of γ-rays energies by HPGe detector

Absolute measurement of γ-ray energies becomes possible after the procedure of energy scale calibration. We use coaxial HPGe detectors for backscattered photons and these detectors are usually located in close proximity of high energy and high current electron/positron beams. Due to unavoidable beams losses, electromagnetic showers produce neutrons in the photo-nuclear reactions and these neutrons can damage the detector, therefore the use of n-type detectors is preferable. As it was already mentioned above, the possibility of precise measurements of γ-rays energies is based on existence of nuclear isotopes with extremely monochromatic γ-radiation [24]. Our application

2017 JINST 12 C08007

requires the knowledge of the energy scale in a wide range, i.e. from hundreds to thousands keV. In table 1 there is a list of the primary calibration sources, which we use for HPGe detector energy scale determination in all of our experiments.

Table 1. The list of primary calibration lines.

Source	Decay half-time, years	γ-rays energies, keV	Reference
^{137}Cs	30.07	661.657 ± 0.003	[25]
^{60}Co	5.27	1173.228 ± 0.003 1332.492 ± 0.004	[25]
^{228}Th (^{208}Tl)	1.91 (3 min)	583.187 ± 0.002 2614.511 ± 0.010	[26]

The radioactive calibration sources are located near the detector as it is shown in figure 1, where the thick arrow represents the beam of laser backscattered photons. The individual adjustment of the counting rate of each calibration γ-source is achieved by varying the distance and insertion of lead plates between the source and the detector.

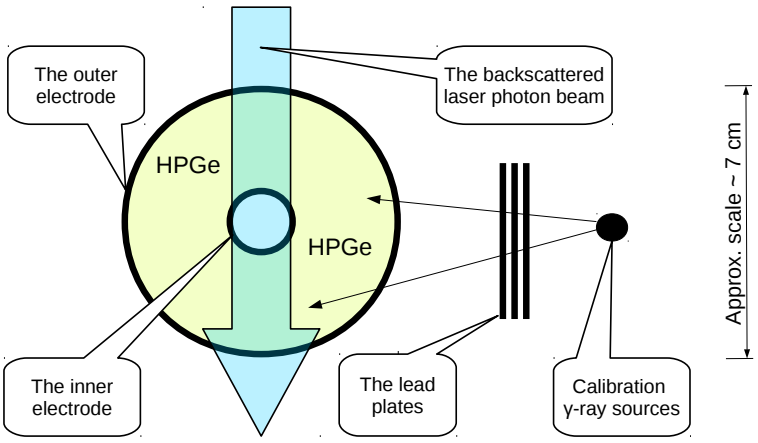

Figure 1. HPGe detector, calibration sources, beam of backscattered photons.

In order to extend our understanding of the detector energy scale towards higher energies, we use the ^{238}Pu/^{13}C source made by RITVERC GmbH.[2] This source of high-energy γ-rays is based on the $^{13}C(\alpha, n) \rightarrow {}^{16}O^*$ reaction with α-particles originating from ^{238}Pu decays (decay half-time is 87.74 years). Excited oxygen via transition to the ground state emits γ-rays with the energy $E_\gamma = 6129$ keV. Per 4π solid angle typical photon/neutron outputs are $2 \cdot 10^3$ s^{-1} and $5 \cdot 10^5$ s^{-1} correspondingly at nominal source activity of 500 mCi.

In table 2 there is a compilation of different results on the subject of precise value of γ-rays energy emitted by this source. In the first line of table 2 the corrected E_γ reflects the present values of mass excess for neutron, ^{2}H and ^{3}H [31]. The correction in the second line is due to the change

[2] www.ritverc.com.

2017 JINST 12 C08007

Table 2. The energy of photons E_γ emitted by $(3^-; 0)$ excited level of ^{16}O.

N	Reaction	Reported energy [keV]	Year, reference	Corrected E_γ [keV]
1	$^{16}\mathrm{N}(\beta^-)^{16}\mathrm{O}$	$E_\gamma = 6129.170 \pm 0.043$	1975, [28]	$E_\gamma = 6129.03 \pm 0.04$
2	$^{13}\mathrm{C}(\alpha, n)^{16}\mathrm{O}$	$E_\gamma = 6129.266 \pm 0.053$	1981, [27]	$E_\gamma = 6129.24 \pm 0.05$
3	$^{19}\mathrm{F}(n, \alpha)^{16}\mathrm{O}$	$E_\gamma = 6129.119 \pm 0.040$	1986, [29]	$E_\gamma = 6129.12 \pm 0.04$
4	$(3^-; 0)$ ^{16}O level	$E_x = 6129.893 \pm 0.040$	1993, [30]	$E_\gamma = 6128.63 \pm 0.04$

in the present reference value of the energy of ^{198}Au γ-rays. Here we would like to mention that the energy E_γ in the last line of table 2 is definitely in contradiction with the values in the first three lines. It is not clear from [30] how this value was obtained and why it is so different.

2.1 The shape of the photopeak

The detector charge-sensitive preamplifier is connected to the digital signal processing unit DSPEC Pro,[3] whose integral and differential nonlinearities are ±250 ppm and ±1% correspondingly according to factory specifications. In order to reduce the influence of electronics nonlinearity (including preamlifier) to our measurements, we use a precision pulse generator PB-5[4] with the integral nonlinearity of ±15 ppm. The PB-5 output is connected by the "test" input to the first cold cascade of preamplifier. The pulser is controlled by a simple computer code, whose role is to switch the pulse amplitudes according to a manually determined table of voltages. The repetition rate of pulses is about 50 Hz and the jumps between different voltages in the table occurs every few seconds.

The response of a γ-ray spectrometer to monochromatic excitation we define as:

$$f(x) = \frac{\sqrt{2/\pi}}{\sigma_R + \sigma_L} \begin{cases} \exp\left(-x^2/2\sigma_R^2\right) & \text{if } x > 0; \\ \exp\left(-x^2/2\sigma_L^2\right) & \text{if } x \le 0. \end{cases} \tag{2.1}$$

Here $x = E - E_{\max}$ is the difference between the energy deposition in the detector and its most probable value. σ_R (right) and σ_L (left) describe the spectrometer resolution including possible asymmetry. The photopeaks from monochromatic radio-nuclide γ-rays in the energy spectrum obtained from HPGe spectrometer are then described by the function:

$$g(x) = B + A \begin{cases} f(x) & \text{if } x => 0; \\ C + (1 - C)f(x) & \text{if } x =\le 0; \end{cases} \tag{2.2}$$

where A is the amplitude and B is the background level. Parameter C describes the influence of low-angle Compton scattering in the material between the source and the detector and depends on calibration setup geometry. Examples of the measured calibration photopeaks with fitting curves are shown in figure. 2. The fit function is defined by eq. (2.2). The energies on the x-axis of the plots is derived from MCA channels according to the linear transformation:

$$E_\gamma \text{ [keV]} = \textbf{zero} \text{ [keV]} + \textbf{gain} \text{ [keV]} \cdot \text{ch}\,, \tag{2.3}$$

where **zero** is the pedestal and **gain** is the calibration coefficient.

[3] www.ortec-online.com.

[4] www.berkeleynucleonics.com/model-pb-5.

2017 JINST 12 C08007

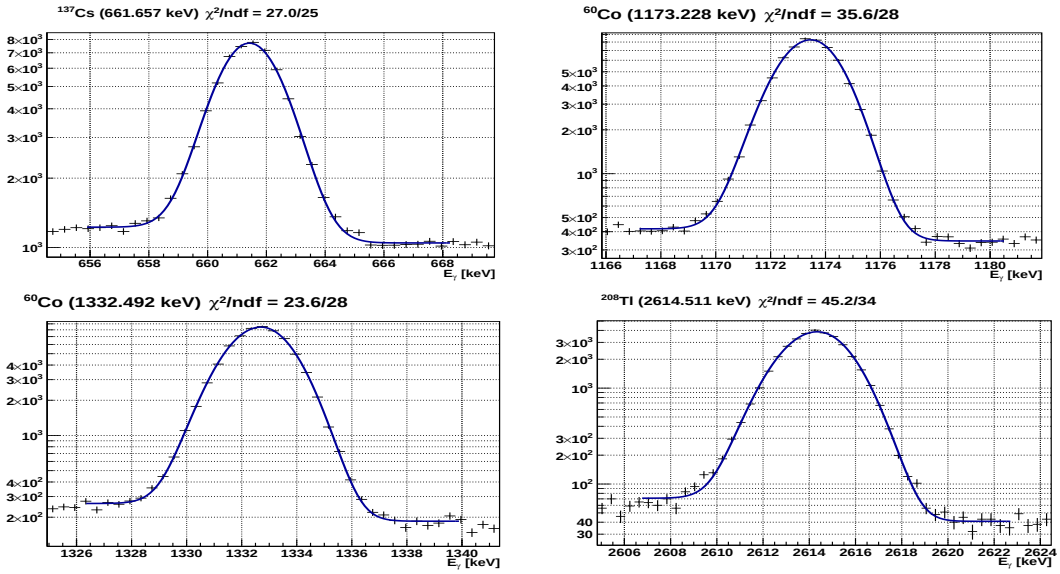

Figure 2. The results of fitting the photopeaks from calibration γ-rays by the function defined in eq. (2.2).

2.2 The energy resolution model

After fitting of all of the γ-peaks founded in the measured energy spectrum, the obtained parameters and their errors are stored inside the internal memory of the analysis software. Figure 3 is the plot of resolution parameters σ_R and σ_L versus E_γ.

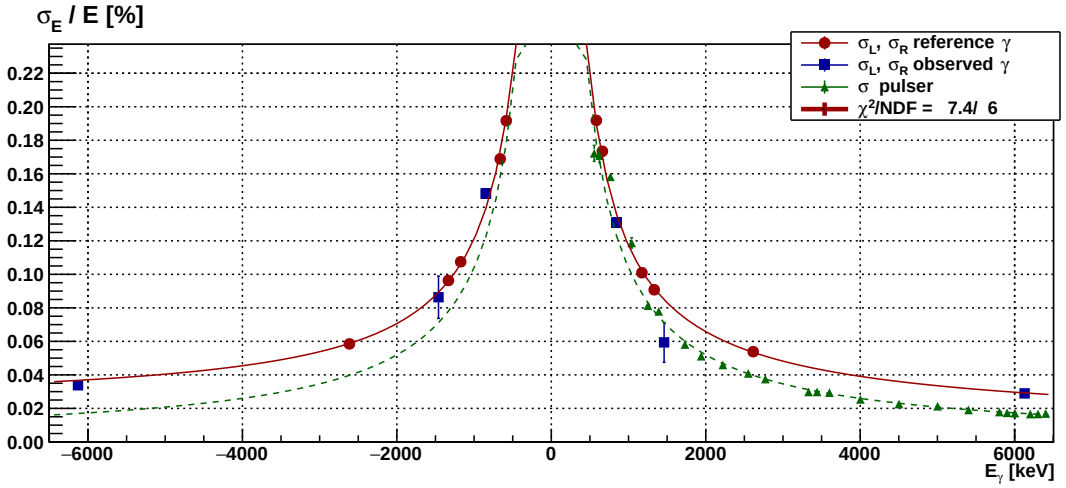

Figure 3. The spectrometer energy resolution. Red circles are from the calibration γ-ray lines listed in table 1. The values of σ_R are drawn at positive energies while the values of σ_L — at negative, just for better visualization. The red solid line is the result of the combined fit by the functions (2.4a) and (2.4b). Blue squares correspond to γ-ray lines not used for calibration, namely ^{40}K 1460 keV line, ^{16}O 6129 keV line from ^{238}Pu/^{13}C source and 847 keV line of ^{56}Co/^{56}Mn, produced in surrounding materials by the neutrons emitted by this source. Green triangles are from pulser calibration peaks: they are fitted by a constant (dashed green line) and have no asymmetry ($\sigma_R = \sigma_L = \sigma_{\text{pulser}}$).

2017 JINST 12 C08007

The σ_R and σ_L dependencies from E_γ are parameterized as follows:

$$\sigma_R = \sqrt{p_0^2 + p_1 \epsilon E_\gamma} \ , \tag{2.4a}$$

$$\sigma_L = \sqrt{p_0^2 + p_1 \epsilon E_\gamma + p_2 (p_3 - E_\gamma)^2} \ , \tag{2.4b}$$

where σ_R and σ_L are in [keV], p_0 is the noise impact to the resolution, $\epsilon = 2.96\,\text{eV}$ is the electron-hole pair creation energy in Ge and p_1 is the dimensionless parameter known as Fano factor [32] (still a free parameter for fitting). The last two parameters, $p_2 > 0$ and p_3 serve for an account of ballistic deficit and charge carrier trapping effects in HPGe, both leading to asymmetric energy response of the spectrometer. A way to account for these effects in eq. (2.4b) was founded empirically. The plots of σ_R and σ_L vs E_γ are fitted by combined fit with common parameters p_0 and p_1. Apparently, positive value of p_3 obtained from the fit indicates substantial contribution of charge carrier trapping effect to the energy response of the spectrometer, i.e. it is a symptom of the neutron damage of the HPGe. It can be concluded from figure 3 that the shape of the 1460 keV line of ^{40}K is not well described by expression (2.2) probably because of rather unclear irradiation geometry. This remark applies even more to the single and double escape peaks (not shown in figure 3) making them impossible to use for scale calibration within this approach. A good coincidence between the result of the fit and the points from 6129 keV line of ^{238}Pu/^{13}C source, not accounted by the fit, shows that the energy resolution model and procedure in whole are strong enough to determine the response function parameters even at high energies.

Figure 4 shows the shapes of one of the pulser peaks (left) and the 6129 keV line photopeak (right). The pulser peaks are fitted by expression (2.2) with $\sigma_R = \sigma_L = \sigma_{\text{pulser}}$, $C = 0$. The 6129 keV line will be used to check our ability of measuring the energies in absolute scale.

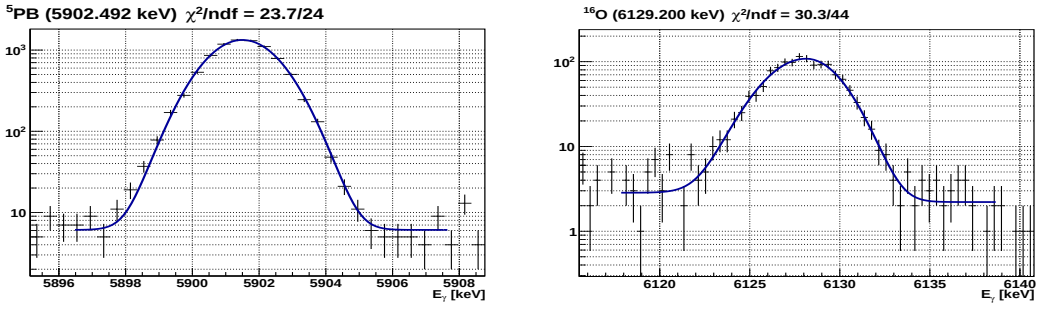

Figure 4. The fits of the "5902 keV" pulser peak (left) and 6129 keV photopeak (right).

2.3 Curved ruler approach for absolute scale determination

Accurate absolute measurement of the γ-rays energies is performed via two steps: a) linear scale calibration with lines from the table 1 and b) correction of the electronics nonlinearity by precision pulser signals. The result of such a procedure is shown in figure 5. First we adjust the bin-to-keV linear conversion parameters (**zero** and **gain** in expr. (2.3)) and redefine the x-axis of the histogram accordingly. The discrepancies between the peaks energies obtained from the fits and corresponding reference energies from table 1 ($E_{\text{FIT}} - E_{\text{REF}}$) are shown vs $E_\gamma = E_{\text{FIT}}$ in figure 5 by red circles.

2017 JINST 12 C08007

The **zero** and **gain** parameters are defined in such a way that linear fit to $(E_{\mathrm{FIT}} - E_{\mathrm{REF}})$ vs E_γ equals zero. The errors bars are defined by both the statistical uncertainties obtained from the fits and the accuracies of the reference energies. These errors define the confidence interval of the absolute energy scale calibration at any certain energy measured by the spectrometer.

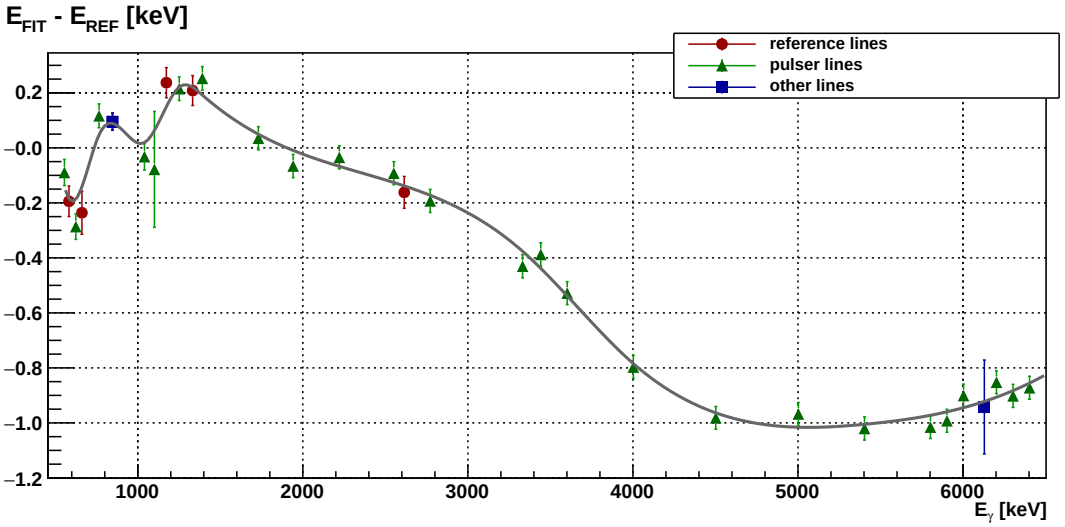

Figure 5. The spectrometer energy scale calibration. Red circles are obtained from the calibration γ-ray lines from table 1. Green triangles are from pulser peaks in the spectrum. Blue squares — see the text below.

As for the pulser lines in the spectrum, we use linear conversion for the set of the pulser amplitudes A_i to corresponding energies: $\mathrm{E}^{(i)}_{\mathrm{REF}}$ [keV] = P_0 [keV] + P_1 [keV/V] · A_i [V]. All of the pulser peaks in the spectrum are fitted (see e.g. figure 4) and the $E^{(i)}_{\mathrm{FIT}}$ energies are assigned to each point. The dependence $(E^{(i)}_{\mathrm{FIT}} - E^{(i)}_{\mathrm{REF}})$ vs $E_\gamma = E^{(i)}_{\mathrm{FIT}}$ is fitted by the univariate spline, see figure 5. Then the P_0 and P_1 parameters are adjusted to minimize the difference between this line and the points of absolute calibration (red circles in figure 5).

The above procedure is based on the assumption that all the integral nonlinearity in energy determination is caused by electronics. We can verify the accuracy of this assumption by application of our procedure for the measurement of a known energy line. In figure 5 there are two points (blue squares) corresponding to the $E_{\mathrm{REF}} = 846.764 \pm 0.002$ keV line of ^{56}Mn/^{56}Co and the $E_{\mathrm{REF}} = 6129.08 \pm 0.04$ keV line of ^{16}O. The former point support our hypothesis: obtained energy shift is perfectly explained by the electronics nonlinearity. The value of E_{REF} for the latter point is taken as the average between the second and the third lines of table 2 while there is no significant contradiction with the first line also. But we are forced to conclude that either our procedure is wrong either the E_{REF} in the last line of table 2 is incorrect.

3 The backscattered laser photons

The energy spectrum of monochromatic laser photons with energy ω_0 backscattered on ultra-relativistic electrons with energy E has singularity near the maximum possible energy ω_{max} defined

2017 JINST 12 C08007

by the relativistic scattering kinematics:

$$\omega_{\max} = E\frac{\kappa}{1+\kappa}\,,\ \text{where}\ \kappa = \frac{4\omega_0 E}{m^2} \tag{3.1}$$

and m is the electron rest energy. However the electrons in the beam have normal energy distribution described by the mean energy E_0 and r. m. s. beam spread parameter σ_E. It will give additional blurriness for the γ-rays energies near $\omega_{\max}$, defined by the derivation of eq. (3.1):

$$\sigma_\omega(\omega_{\max}) = \frac{(2+\kappa)\kappa}{(1+\kappa)^2}\sigma_E. \tag{3.2}$$

The joint effect of the normal distribution with the mean value of photon energy $\omega_{\max}(E_0)$ and r. m. s. width $\sigma_\omega(\omega_{\max})$ and the asymmetric spectrometer response function (eq. (2.1)) is defined by their convolution. It can be calculated analytically:

$$S(x) = \frac{\exp\left(\frac{-x^2/2}{\sigma_R^2+\sigma_\omega^2}\right)\operatorname{erfc}\left(\frac{-x\sigma_R/\sigma_\omega}{\sqrt{2(\sigma_R^2+\sigma_\omega^2)}}\right)}{(1+\sigma_L/\sigma_R)\sqrt{2\pi(\sigma_R^2+\sigma_\omega^2)}} + \frac{\exp\left(\frac{-x^2/2}{\sigma_L^2+\sigma_\omega^2}\right)\operatorname{erfc}\left(\frac{x\sigma_L/\sigma_\omega}{\sqrt{2(\sigma_L^2+\sigma_\omega^2)}}\right)}{(1+\sigma_R/\sigma_L)\sqrt{2\pi(\sigma_L^2+\sigma_\omega^2)}}\,, \tag{3.3}$$

where $x = E_\gamma - \omega_{\max}(E_0)$. In case when the laser wave is scattered on a free electron (e.g. at VEPP-4M and BEPC-II) with a certain energy E, the energy spectrum of backscattered laser photons is described as:

$$F(x) = A(1 + A'x + A''x^2)\int_x^\infty \delta(y)dy + H(1 + H'x), \tag{3.4}$$

where $\delta(y)$ is the Dirac delta function. Amplitudes A, A' and A'' are introduced in order to account for laser-electron beams scattering intensity, differential cross section near $x = 0$, Compton scattering of backscattered photons in the materials between the scattering area and the detector, detector efficiency and its slope, out-of-photopeak counts, etc. Amplitudes H and H' describe the hard beam background radiation unrelated to laser backscattering. In case when the laser-electron interaction occurs inside the bending magnet with the transverse magnetic induction B (the case at VEPP-2000), the spectrum shape near $\omega_{\max}$ is more complex. For the explanation please refer to [23] while here we use the final result of those considerations to describe the spectrum shape:

$$G(x) = A(1 + A'x + A''x^2)\int_z^\infty \mathrm{Ai}(y)dy + H(1 + H'x), \tag{3.5}$$

where $\mathrm{Ai}(y)$ is the Airy function. The meanings of A and H amplitudes are the same as in eq. (3.4) and variable z is defined as

$$z = \xi^{\frac{2}{3}}\left((u/\kappa)^{\frac{2}{3}} - (\kappa/u)^{\frac{1}{3}}\right),\ \text{where}\ \xi = 4\frac{\omega_0}{m}\frac{B_0}{B},\quad u = \frac{E_\gamma}{E_0 - E_\gamma}\ \text{and}\ \kappa = \frac{4\omega_0 E_0}{m^2}. \tag{3.6}$$

The constant parameter $B_0 = 4.414 \cdot 10^9$ [T] is the Schwinger field strength.

2017 JINST 12 C08007

When the free electron is scattered ($B = 0$, the case of VEPP-4M and BEPC-II) the fit of the edge of the energy spectrum of backscattered laser photons is performed by the convolution of eqs. (3.3) and (3.4): $N(x) = F(x) * S(x)$. The parameters σ_R and σ_L are fixed during fitting and obtained from the results of the calibration of γ-ray spectrometer energy resolution (figure 3). The $\omega_{\max}$, σ_ω, A, A', A'', H, H' are free parameters and their values are obtained from the fit results. The values of E_0 and σ_E are obtained from $\omega_{\max}$ and σ_ω using the relations (3.1) and (3.2).

When $B \neq 0$ (like at the VEPP-2000), the fit is performed by the convolution of eqs. (3.3) and (3.5): $N(x) = G(x) * S(x)$. The only difference from the previous case is that E_0 and B become the parameters of the fit function and their values are obtained directly from the fit results. The examples for both cases are presented in figure 6, including the corresponding experimental spectra, fit functions and the results of the mean beam energy and beam energy spread determination.

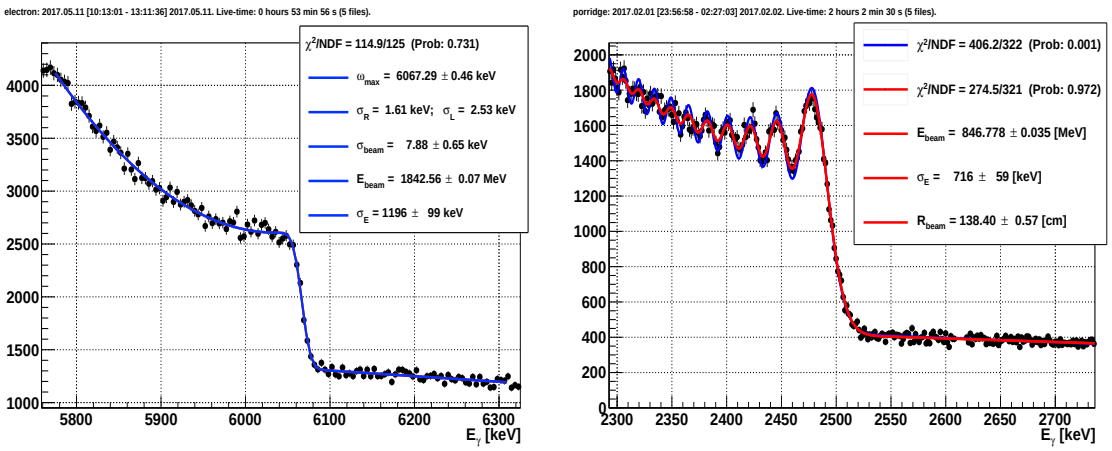

Figure 6. The fits of the edges of the spectra of backscattered laser photons. The one on the left was obtained at the BEPC-II collider using CO_2 laser radiation with wavelength in vacuum $\lambda = 10.591035\mu$m. The one on the right was obtained at the VEPP-2000 collider using CO laser radiation with wavelength in vacuum $\lambda = 5.426463\mu$m.

4 Conclusion

We have described our experience of the absolute beam energy measurement in colliders by the laser backscattering approach. The procedure of HPGe detector energy scale calibration is based on the nuclear sources of γ-rays while the nonlinearity of the electronics is corrected by precision pulser. This approach could be considered as the accurate energy scale transfer from optics (laser radiation wavelengths, $\sim$ eV scale) through the nuclear spectroscopy (nuclear γ-ray sources for detector calibration, $\sim$ MeV scale) to the scale of particle masses in the range up to $\sim$ 2 GeV. Achieved accuracy of beam energy determination at three lepton colliders is not worse than 50 keV.

Acknowledgments

This work was supported by Russian Science Foundation (project N 14-50-00080).

2017 JINST 12 C08007

References

[1] I.C. Hsu, C.C. Chu and C.I. Yu, *Energy measurement of relativistic electron beams by laser Compton scattering*, *Phys. Rev.* **E 54** (1996) 5657.

[2] H. Ohkuma, M. Shoji, S. Suzuki, K. Tamura, T. Yorita, K. Nakayama et al., *Production of MeV photons by the laser Compton scattering using a far infrared laser at SPring-8*, in *Proceedings of EPAC*, 2006, pp. 961–963.

[3] R. Klein, R. Thornagel, G. Ulm, T. Mayer and P. Kuske, *Beam diagnostics at the BESSY I electron storage ring with Compton backscattered laser photons: Measurement of the electron energy and related quantities*, *Nucl. Instrum. Meth.* **A 384** (1997) 293.

[4] R. Klein, R. Thornagel, G. Brandt, G. Ulm, P. Kuske and R. Gorgen, *Measurement of the BESSY II electron beam energy by Compton-backscattering of laser photons*, *Nucl. Instrum. Meth.* **A 486** (2002) 545.

[5] C. Sun, J. Li, G. Rusev, A.P. Tonchev and Y.K. Wu, *Energy and energy spread measurements of an electron beam by Compton scattering method*, *Phys. Rev. ST-Accel. Beams* **12** (2009) 1.

[6] K. Horikawa, S. Miyamoto, S. Amano and T. Mochizuki, *Measurements for the energy and flux of laser Compton scattering γ-ray photons generated in an electron storage ring: NewSUBARU*, *Nucl. Instrum. Meth.* **A 618** (2010) 209.

[7] C. Chang et al., *First results of energy measurements with a compact Compton backscattering setup at ANKA*, in *Proceedings of the 6th International Particle Accelerator Conference (IPAC 2015)*, 2015, pp. 876-878.

[8] O.V. Anchugov et al., *Experiments on the physics of charged particle beams at the VEPP-4M electron-positron collider*, *J. Exp. Theor. Phys.* **109** (2009) 590.

[9] Q. Qing, H. Nan, L. Wei-Bin, L. Yu-Dong, P. Yue-Mei, Q. Jing et al., *Beam dynamics studies on BEPC-II storage rings at the commissioning stage*, *Chin. Phys.* **C 33** (2009) 65.

[10] D.E. Berkaev, D.B. Shwartz, P.Y. Shatunov, Y.A. Rogovskii, A.L. Romanov, I.A. Koop et al., *The VEPP-2000 electron-positron collider: First experiments*, *J. Exp. Theor. Phys.* **113** (2011) 213.

[11] V.E. Blinov, V.V. Kaminsky, E.B. Levichev, N.Yu. Muchnoi, S.A. Nikitin, I.B. Nikolaev et al., *Beam energy and energy spread measurement by Compton backscattering of laser radiation at the VEPP-4M collider*, *ICFA Beam Dynamics Newsletters* **48** (2009) 195.

[12] G.Ya. Kezerashvili, A.M. Milov, N.Yu. Muchnoi and A.P. Usov, *A Compton source of high-energy polarized tagged gamma-ray beams. The ROKK-1M facility*, *Nucl. Instrum. Meth.* **B 145** (1998) 40.

[13] V.V. Anashin et al., *Measurement of the tau lepton mass at the KEDR detector*, *JETP Lett.* **85** (2007) 347.

[14] A.N. Skrinsky and Yu.M. Shatunov, *Precision measurements of masses of elementary particles using storage rings with polarized beams*, *Sov. Phys. Usp.* **32** (1989) 548.

[15] V.V. Anashin et al., *The KEDR detector*, *Phys. Part. Nucl.* **44** (2013) 657.

[16] V.E. Blinov, A.V. Bogomyagkov, N. Yu. Muchnoi, S.A. Nikitin, I.B. Nikolaev, A.G. Shamov et al., *Review of beam energy measurements at VEPP-4M collider: KEDR/VEPP-4M*, *Nucl. Instrum. Meth.* **A 598** (2009) 23.

[17] E.V. Abakumova et al., *The Beam energy measurement system for the Beijing electron-positron collider*, *Nucl. Instrum. Meth.* **A 659** (2011) 21 [arXiv:1109.5771].

2017 JINST 12 C08007

[18] E.V. Abakumova, M.N. Achasov, A.A. Krasnov, N. Yu. Muchnoi and E.E. Pyata, *The system for delivery of IR laser radiaton into high vacuum*, 2015 *JINST* **10** T09001 [arXiv:1504.00130].

[19] J.-Y. Zhang et al., *Upgrade of Beam Energy Measurement System at BEPC-II*, *Chin. Phys.* **C 40** (2016) 076001 [arXiv:1510.08167].

[20] V.V. Anashin et al., *Final analysis of KEDR data on J/ψ and $\psi(2S)$ masses*, *Phys. Lett.* **B 749** (2015) 50.

[21] BESIII collaboration, M. Ablikim et al., *Precision measurement of the mass of the τ lepton*, *Phys. Rev.* **D 90** (2014) 012001 [arXiv:1405.1076].

[22] E.V. Abakumova et al., *A system of beam energy measurement based on the Compton backscattered laser photons for the VEPP-2000 electron-positron collider*, *Nucl. Instrum. Meth.* **A 744** (2014) 35 [arXiv:1310.7764].

[23] E.V. Abakumova, M.N. Achasov, D.E. Berkaev, V.V. Kaminsky, N. Yu. Muchnoi, E.A. Perevedentsev et al., *Backscattering of Laser Radiation on Ultrarelativistic Electrons in a Transverse Magnetic Field: Evidence of MeV-Scale Photon Interference*, *Phys. Rev. Lett.* **110** (2013) 140402 [arXiv:1211.0103].

[24] R. Helmer and C. van der Leun, *Recommended standards for γ-ray energy calibration (1999)*, *Nucl. Instrum. Meth.* **A 450** (2000) 35.

[25] M.-M. Bé, V. Chisté, C. Dulieu, E. Browne, V. Chechev, N. Kuzmenko et al., *Table of Radionuclides*, Monographie BIPM-5, vol. 4, Bureau International des Poids et Mesures, Pavillon de Breteuil, F-92310 Sèvres, France, 2008.

[26] M.-M. Bé, V. Chisté, C. Dulieu, E. Browne, V. Chechev, N. Kuzmenko et al., *Table of Radionuclides*, Monographie BIPM-5, vol. 2, Bureau International des Poids et Mesures, Pavillon de Breteuil, F-92310 Sèvres, France, 2004.

[27] P. Alkemade, C. Alderliesten, P. D. Wit and C. V. der Leun, *The energy of the 6.13 MeV γ-transition in ^{16}O related to the gold standard*, *Nucl. Instrum. Meth.* **197** (1982) 383.

[28] E.B. Shera, *Measurement of the energy of the 6129-keV gamma ray of O-16*, *Phys. Rev.* **C 12** (1975) 1003.

[29] T. Kennett, W. Prestwich and J. Tsai, *Energy determination of the 6129 keV ^{16}O transition*, *Nucl. Instrum. Meth. A* **247** (1986) 420.

[30] DD.R. Tilley, H.R. Weller and C.M. Cheves, *Energy levels of light nuclei A = 16-17*, *Nucl. Phys.* **A 564** (1993) 1.

[31] G. Audi, F.G. Kondev, M. Wang, W.J. Huang and S. Naimi, *The NUBASE2016 evaluation of nuclear properties*, *Chin. Phys.* **C 41** (2017) 030001.

[32] U. Fano, *On the theory of ionization yield of radiations in different substances*, *Phys. Rev.* **70** (1946) 44.

2017 JINST 12 C08007